Cell Host & Microbe
Resource

Systematic Analysis of Viral and Cellular MicroRNA Targets in Cells Latently Infected with Human γ-Herpesviruses by RISC Immunoprecipitation Assay

Lars Dölken,[1,9] Georg Malterer,[1,9] Florian Erhard,[2] Sheila Kothe,[1] Caroline C. Friedel,[2] Guillaume Suffert,[3] Lisa Marcinowski,[1] Natalie Motsch,[4] Stephanie Barth,[4] Michaela Beitzinger,[5] Diana Lieber,[1] Susanne M. Bailer,[1] Reinhard Hoffmann,[6] Zsolt Ruzsics,[1] Elisabeth Kremmer,[7] Sébastien Pfeffer,[3] Ralf Zimmer,[2] Ulrich H. Koszinowski,[1] Friedrich Grässer,[4] Gunter Meister,[5] and Jürgen Haas[1,8,*]

[1]Max von Pettenkofer-Institute, Ludwig-Maximilians-University Munich, Pettenkofer Strasse 9a, 80336 Munich, Germany
[2]Institute for Informatics, Ludwig-Maximilians-University Munich, Amalienstrasse 17, 80333 Munich, Germany
[3]Institut de Biologie Moléculaire et Cellulaire du CNRS, 15 rue René Descartes, Université de Strasbourg, 67084 Strasbourg, France
[4]Institute of Virology, Haus 47, Universitätsklinikum des Saarlandes, 66421 Homburg/Saar, Germany
[5]Max Planck Institute of Biochemistry, Am Klopferspitz 18, 82152 Martinsried, Germany
[6]Institute of Medical Microbiology, Technical University Munich, Trogerstrasse 30, 81675 Munich, Germany
[7]Helmholtz Zentrum München, Institut für Molekulare Immunologie, Marchioninistraße 25, 81377 Munich, Germany
[8]Division of Pathway Medicine, University of Edinburgh, 49 Little France Crescent, Edinburgh EH16 4SB, UK
[9]These authors contributed equally to this work
*Correspondence: haas@lmb.uni-muenchen.de
DOI 10.1016/j.chom.2010.03.008

SUMMARY

The mRNA targets of microRNAs (miRNAs) can be identified by immunoprecipitation of Argonaute (Ago) protein-containing RNA-induced silencing complexes (RISCs) followed by microarray analysis (RIP-Chip). Here we used Ago2-based RIP-Chip to identify transcripts targeted by Kaposi's sarcoma-associated herpesvirus (KSHV) miRNAs (n = 114), Epstein-Barr virus (EBV) miRNAs (n = 44), and cellular miRNAs (n = 2337) in six latently infected or stably transduced human B cell lines. Of the six KSHV miRNA targets chosen for validation, four showed regulation via their 3′UTR, while two showed regulation via binding sites within coding sequences. Two genes governing cellular transport processes (TOMM22 and IPO7) were confirmed to be targeted by EBV miRNAs. A significant number of viral miRNA targets were upregulated in infected cells, suggesting that viral miRNAs preferentially target cellular genes induced upon infection. Transcript half-life both of cellular and viral miRNA targets negatively correlated with recruitment to RISC complexes, indicating that RIP-Chip offers a quantitative estimate of miRNA function.

INTRODUCTION

Herpesviruses are large DNA viruses which after primary infection persist for life, leaving the infected individual at risk for reactivation and subsequent disease. They are divided into three subfamilies based on sequence homologies and unique biological features (α-, β-, and γ-herpesviruses). Humans are infected with two members of the γ-herpesvirus family, namely Kaposi's sarcoma-associated herpesvirus (KSHV) and Epstein-Barr virus (EBV). Both infect B cells and can induce proliferative diseases in humans (Barozzi et al., 2007). KSHV is involved in the development of several human tumors, including Kaposi's sarcoma, primary effusion lymphoma (PEL), and multicentric Castleman disease (reviewed in Dourmishev et al., 2003; Schulz, 2006). PEL tumor cells are thought to originate from postgerminal center B cells due to the presence of hypermutated immunoglobulin genes (Gaidano et al., 1997) and display an intermediate immunophenotype between immunoblasts and plasma cells (Carbone et al., 1996; Nador et al., 1996). The cell line body cavity-based lymphoma-1 (BCBL-1) was established from a malignant effusion (Renne et al., 1996) and serves as a model cell line for PEL. Four groups independently reported on 12 miRNAs expressed during latent infection in PEL cells (Cai et al., 2005; Grundhoff et al., 2006; Pfeffer et al., 2005; Samols et al., 2005), which are remarkably conserved among isolates from many different clinical sources (Marshall et al., 2007).

EBV has been linked to various human malignancies including Burkitt's and Hodgkin's lymphoma, NK/T cell and peripheral T cell lymphoma, posttransplant lymphoma, and nasopharyngeal and gastric carcinoma and is responsible for posttransplant lymphoproliferative disease (PTLD) (Delecluse et al., 2007). EBV readily transforms primary human B-lymphocytes which are the in vitro correlate of EBV-associated PTLD arising under severe immunosuppression (Carbone et al., 2008). EBV encodes for at least 25 miRNAs derived from three separate miRNA clusters (Cai et al., 2006; Grundhoff et al., 2006; Pfeffer et al., 2004; Zhu et al., 2009).

Since viral miRNAs were first described in 2004 (Pfeffer et al., 2004), only very few targets have been identified. For KSHV these include targets involved in angiogenesis, proliferation, immune evasion, or repression of apoptosis (Gottwein et al., 2007; Nachmani et al., 2009; Samols et al., 2007; Skalsky

et al., 2007; Ziegelbauer et al., 2009). In addition, EBV miRNAs promote cell survival (Choy et al., 2008) and target cellular chemokines (CXCL-11) (Xia et al., 2008). Similar to human cytomegalovirus miR-UL112-1, both kshv-miR-K12-7 and ebv-miR-BART2 target MICB, an activating stress-induced NK cell ligand involved in immune recognition of infected cells (Nachmani et al., 2009; Stern-Ginossar et al., 2007).

Recently, immunoprecipitation of RISCs followed by microarray analysis of the RISC-bound miRNA targets (RIP-Chip) was shown to permit the identification of hundreds of cellular miRNA targets with high specificity (Baroni et al., 2008; Beitzinger et al., 2007; Easow et al., 2007; Hendrickson et al., 2008; Karginov et al., 2007; Keene et al., 2006). Here we applied Argonaute 2 (Ago2)-RIP-Chip to identify both cellular and viral miRNA targets in six human B cell lines. We report on the identification of 2337 putative targets of cellular and 158 targets of viral miRNAs in human B cells. Thus, we provide a comprehensive atlas of cellular miRNA targets in human B cells and extend the list of cellular targets of all viral miRNA targets identified so far by > 5-fold.

RESULTS

Study Design

Cellular targets of human γ-herpesvirus miRNAs in B cells were identified by immunoprecipitation (IP) of RISCs followed by microarray analysis of the coimmunoprecipitated mRNAs (RIP-Chip). To identify KSHV miRNA targets, we used the KSHV-positive cell line BCBL-1 and the KSHV- and EBV-negative cell line DG75 transduced by a lentiviral vector to stably express the ten intronic KSHV miRNAs (DG75-10/12). DG75 transduced with eGFP (DG75-eGFP) served as control (Wang et al., 2004). To identify viral miRNA targets of EBV, the prototype B95.8 strain of EBV (BL41 B95.8) and its parental Burkitt's lymphoma cell line (BL41) were used. As B95.8 has lost more than half of the viral miRNAs (Cai et al., 2006), the Jijoye cell line featuring a nondeleted strain, where all known EBV miRNAs are present (Grundhoff et al., 2006), was included.

Identification of Cellular miRNA Targets in Human B Cells

We established a protocol for RISC IP in human B cells using the recently described monoclonal antibody to human Ago2 (α-hAgo2; 11A9) (Rudel et al., 2008). A monoclonal antibody against bromodesoxyuridine (BrdU) served as control. In all experiments the efficiency of the IP was analyzed by quantitative PCR. Usually, an ~1000-fold (670- to 3300-fold) enrichment of cellular Let7a levels was observed when comparing the Ago2-IP with the BrdU-IP samples. A consistent recovery rate of ~50% of Let7a was observed, indicating that Ago2-bound miRNAs comprise at least half of the cellular miRNA pool in human B cells (see Figure S1 available online). Enrichment of cyclin E1 mRNA (CCNE1), a cellular miRNA target of both hsa-miR-16 and hsa-miR-15a (Bandi et al., 2009; Liu et al., 2008), served as a positive control. It was typically enriched by ~8-fold.

Next, microarray analyses of two independent biological replicates for each cell line were performed using Affymetrix human Gene ST 1.0 arrays. For DG75-eGFP, DG75-10/12, and BCBL-1, both the α-Ago2-IP and the α-BrdU-IP samples were analyzed. For both BL41 and BL41 B95.8, the amounts of RNA obtained by the α-BrdU-IPs were too small (50–100 ng) for microarray analysis using the same experimental setting and microarray platform. As the control IP is thought to merely represent total RNA levels in the cell and total RNA has been successfully used as control for the Ago2-IP (Weinmann et al., 2009), we analyzed total RNA instead of the α-BrdU-IP sample for BL41, BL41 B95.8, and Jijoye. Enrichment of transcripts in the Ago2-IP was highly concordant for all six human B cell lines irrespective of whether total RNA or the α-BrdU-IP sample was used (Pearson's correlation coefficient between 0.34 and 0.96 for all combinations, $p < 2.2 \times 10^{-16}$). The complete set of data is provided in Table S1.

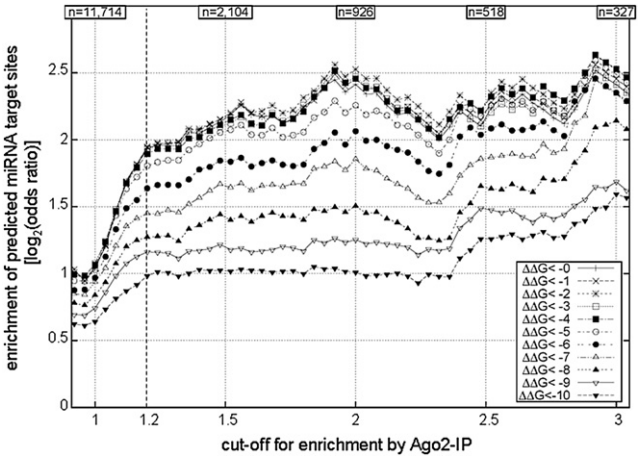

Figure 1. Overrepresentation of Predicted Binding Sites for Cellular miRNAs

Binding sites for these 44 cellular miRNAs expressed in human B cells (Landgraf et al., 2007) were predicted using PITA software and different cutoffs for free binding energies (ΔΔG) ranging from 0 to −10 kcal/mol. Odds ratios for predicted miRNA-binding sites are shown for all genes with a mean enrichment in the Ago2-IP versus control across all six cell lines greater than the indicated value. For each value, the number of transcripts with a mean enrichment greater than this cutoff is shown.

To test for overrepresentation of predicted miRNA-binding sites of cellular miRNAs among the enriched transcripts, we obtained 44 cellular miRNAs expressed in BL41, BL41 B95.8, and DG75 from the miRNA expression atlas (Landgraf et al., 2007) (Table S2A). We used the miRNA target prediction program PITA (Kertesz et al., 2007) and different ΔΔG cutoff values ranging from 0 to −10 kCal/mol to test for overrepresentation of favorable target sites of any of these miRNAs in target 3′UTRs (Figure 1). Overrepresentation was highly significant down to very low mean enrichments ($p < 10^{-58}$ for a mean enrichment of 1.2-fold). Based on statistical analysis, we identified 2337 transcripts significantly enriched across all six B cell lines ($p < 0.05$, one-sided paired t test) with a mean enrichment > 1.2-fold. Enrichment of their transcripts in the six cell lines is shown in Figure 2A, and a complete list is provided in Table S2B. For these genes, predicted binding sites were significantly overrepresented within 5′UTRs ($p = 8.59 \times 10^{-3}$), coding sequences ($p = 2.02 \times 10^{-27}$), and 3′UTRs ($p = 6.19 \times 10^{-63}$, Fisher's exact test and ΔΔG < −4 kCal/mol, see also Table S3A).

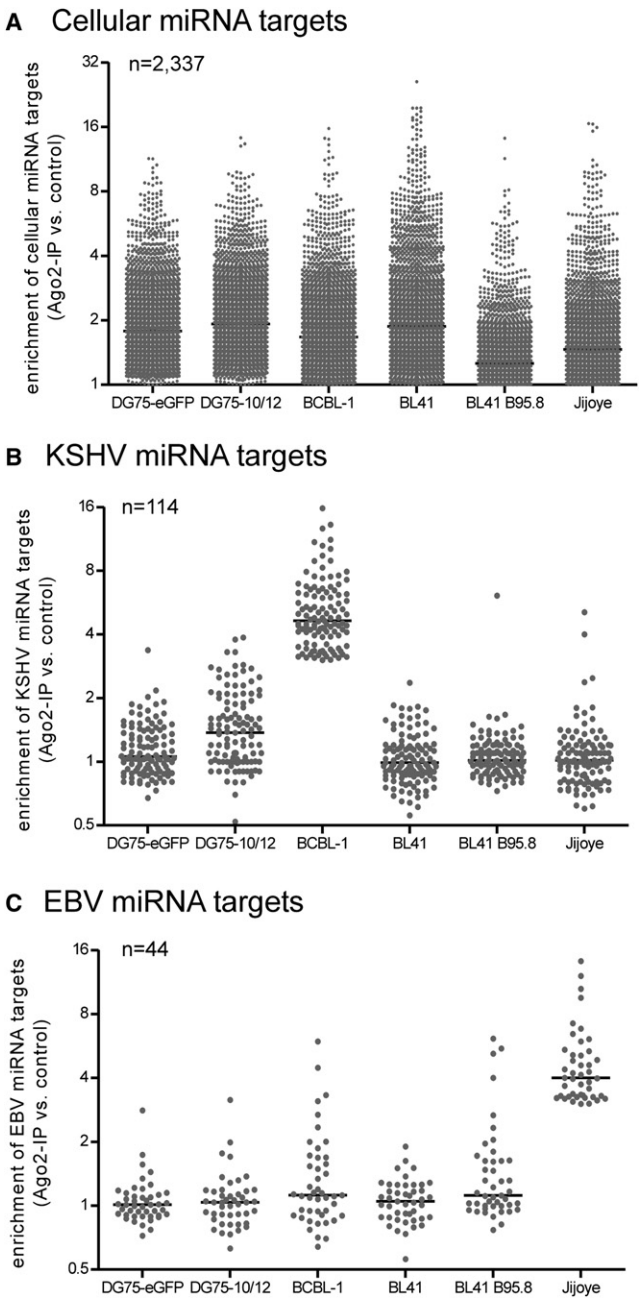

Figure 2. Enrichment of miRNA Targets by RISC Immunoprecipitation

Enrichment of cellular (A, n = 2337), KSHV (B, n = 114), and EBV (C, n = 44) miRNA targets in the Ago2-IPs of the six cell lines under study is shown.

Identification of Viral miRNA Targets

Targets of viral miRNAs may either be exclusively targeted by viral miRNAs or also be targeted by cellular miRNAs. In the first case, their transcripts should only be enriched in the cell lines expressing the viral miRNAs, but not in the two control cell lines DG75-eGFP and BL41. For transcripts targeted by both cellular and viral miRNAs, enrichment in BCBL-1 or Jijoye should be substantially greater than in the two control cell lines. In order to exclude false positives, we defined stringent criteria for a transcript to be considered a KSHV or EBV miRNA target. Enrichment in either BCBL-1 or Jijoye had to be > 3.0 and enrichment in both DG75-eGFP and BL41 < 1.2. For targets of cellular miRNAs (enriched > 1.2-fold in DG75-eGFP and/or BL41), a > 3-fold greater enrichment in BCBL-1 or Jijoye than in both DG75-eGFP and BL41 was required. Enrichment of the 114 KSHV and the 44 EBV putative miRNA targets which fulfilled these criteria are shown in Figures 2B and 2C, respectively. Interestingly, no transcripts were enriched > 3-fold in either DG75-10/12 or BL41 B95.8 and < 1.2-fold in DG75-eGFP and BL41, which were not also enriched > 3-fold in BCBL-1 or Jijoye, respectively. This most likely reflects the reduced levels of viral miRNAs in DG75-10/12 (see Figures S2A and S2B) and BL41 B95.8.

False-positive viral miRNA targets may result from both cellular miRNAs and cellular transcripts induced upon infection. On the one hand, cellular miRNAs induced upon infection may mimic the effect of the viral miRNAs. While little is known about the effect of KSHV infection on cellular miRNA expression, EBV infection has been shown to result in induction of a number of cellular miRNAs, including hsa-miR-155, hsa-miR-146a, and hsa-miR-21 (Gatto et al., 2008; Mrazek et al., 2007). Out of 17 confirmed targets of hsa miR-155 (Gottwein et al., 2007; Skalsky et al., 2007; Vigorito et al., 2007), we noted six (BACH1, FOS, IKBKE, RFK, RPS6KA3 [Gottwein et al., 2007] and SPI1 [Vigorito et al., 2007]) to be enriched between 1.4- and 2.7-fold in Jijoye (Table S3B). This is consistent with significant repression of hsa-miR-155 targets upon EBV infection (Gatto et al., 2008). Still, none of them fulfilled our more stringent criteria. In addition, none of the 12 targets of hsa-miR-21 identified by Yang et al. (Yang et al., 2009b) and none of the four targets of hsa-miR146a (Pauley et al., 2008; Tang et al., 2009) were enriched > 1.5-fold in any of the six cell lines. Thus, we believe that induction of cellular miRNAs did not significantly corrupt our list of EBV miRNA targets.

On the other hand, virus infection may result in the induction of genes that are then targeted by cellular miRNAs. If expression levels are below the detection limit of the microarrays in uninfected B cells, this would present as a selective enrichment of their transcripts in the Ago2-IP in the infected cells; i.e., they would be misinterpreted to be viral miRNA targets. Therefore, we distinguished noninduced targets (KSHV, n = 72; EBV, n = 26; see Tables S4A and S4B) from targets that showed >1.5-fold higher expression levels in the BrdU-IPs of BCBL-1 compared to DG75-eGFP or in total RNA levels of Jijoye when compared to BL41 (KSHV, n = 42; EBV, n = 18; see Tables S4C and S4D). To investigate whether these genes are indeed targeted by viral miRNAs, we studied the overrepresentation of predicted viral miRNA target sites among both the noninduced and induced targets using the PITA algorithm. Indeed, predicted target sites of viral miRNAs were significantly overrepresented in the 3′UTRs and, to a lesser extent, in the 5′UTRs among both the induced and noninduced KSHV and EBV miRNA targets (Tables S3A, S5A, and S5B). Therefore, we concluded that also the majority of the genes induced > 1.5-fold in either BCBL-1 or Jijoye are indeed targets of viral miRNAs.

Validation of Viral miRNA Targets by TaqMan PCR

We representatively validated miRNA targets identified by RIP-Chip analysis using quantitative TaqMan PCR (qPCR). We

randomly chose 11 KSHV miRNA targets that were also enriched > 1.5-fold in DG75-10/12. In addition, we chose eight EBV miRNA targets as well as four well-described targets of cellular miRNAs. Three of the eight EBV miRNA targets (IPO7, TRIM32, and FBXO9) were enriched > 1.5-fold in BL41 B95.8. The rest (n = 5) were not enriched in BL41 B95.8 (enrichment = 0.77–0.96). New RISC-IPs were performed for all six cell lines using two independent biological replicates. Quantitative PCR was performed, and expression levels were normalized to hypoxanthine-guanine phosphoribosyltransferase (HPRT), a commonly used housekeeping gene (Fu et al., 2009), found not to be enriched in our Ago2-IPs. The noncoding RNA H19 (Weinmann et al., 2009) and cyclin E1 mRNA (CCNE1) served as quantitative positive controls (Figures 3A and 3B). Enrichment was significant for 9 of the 11 KSHV miRNA targets in both DG75-10/12 and BCBL-1. ZNF684 was significantly enriched only in BCBL-1. All EBV miRNA targets (8/8 = 100%) were significantly enriched in Jijoye. Significant enrichment in BL41 B95.8 was also observed for IPO7 and TRIM32. Recently, the activating NK cell ligand MICB was found to be targeted by both ebv-miR-BART2-5p, kshv-miR-K12-7 (Nachmani et al., 2009) and hcmv-miR-UL112-1 (Stern-Ginossar et al., 2007). In contrast, MICA, a closely related NK cell ligand, is predominantly targeted by cellular miRNAs (Stern-Ginossar et al., 2008). MICB was enriched significantly stronger in both BL41 B95.8 and Jijoye than in BL41, consistent with ebv-miR-BART2-5p being one of the EBV miRNAs still expressed in BL41 B95.8. Enhanced enrichment of MICB in BCBL-1 was less pronounced but nevertheless detectable. In summary, 18 of 19 (95%) of the viral miRNA targets we tested by qPCR were confirmed.

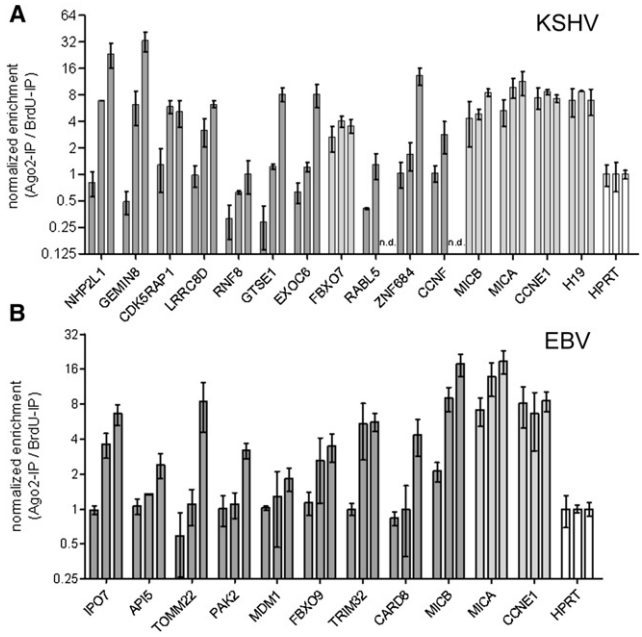

Figure 3. Validation of KSHV and EBV miRNA Targets by qPCR

(A) For each gene, mRNA enrichment (Ago2-IP versus control-IP) normalized for HPRT expression levels is shown for DG75-eGFP (left), DG75-10/12 (middle), and BCBL-1 (right).

(B) For each gene, mRNA enrichment (Ago2-IP versus control-IP) normalized for HPRT expression levels is shown for BL41 (left), BL41 B95.8 (middle), and Jijoye (right). Transcripts with significant enrichment in cells expressing viral miRNAs are indicated in dark gray and cellular miRNA targets in light gray. MICA, CCNE1, and H19, which are known to be targeted by cellular miRNAs, were used as controls. Values represent the mean ± SD of two independent experiments performed in duplicate.

Validation of KSHV miRNA Target Candidates by Dual-Luciferase Assays

In order to experimentally validate viral miRNA targets identified by RIP-Chip and confirmed by qPCR, we cloned the full-length 3′UTRs of 6 of the 11 putative KSHV miRNA targets into a GATEWAY-compatible derivative of the dual-luciferase vector pSIcheck. This vector constitutively expresses renilla and firefly luciferase. Expression of the latter is regulated by the subcloned 3′UTR. KSHV miRNAs were expressed by cotransfection of pcDNAmiR10/12, a vector encoding the ten intronic KSHV miRNAs with the reporter constructs, and luciferase assays were performed 16 hr later. While no effect of KSHV miRNA expression was detectable for the 3′UTR reporter constructs of NHP2L1 and GEMIN8, significant suppression of firefly luciferase expression was detectable for the other four candidates in three independent experiments (Figure 4A). The strongest inhibition was exerted on the LRRC8D reporter (~50%) construct, while the effect on CDK5RAP1 was rather small (~15%) but nevertheless reproducible and significant.

LRRC8D Is Regulated by kshv-miR-K12-3 through a Single Target Site in Its 3′UTR

LRRC8D is a leucin-rich type III transmembrane protein thought to be involved in proliferation and activation of lymphocytes and macrophages. Modeling of possible hybrids between the LRRC8D 3′UTR and the KSHV-encoded miRNAs suggested a strong interaction of the 3′UTR with kshv-miR-K12-3 (Figure 4B, Table S6A). To test whether expression of kshv-miR-K12-3 alone was responsible for the downregulation of luciferase activity in the LRRC8D 3′UTR reporter construct, we performed derepression assays by using a 2′-O-methyl RNA complementary to kshv-miR-K12-3. The inhibition of kshv-miR-K12-3 resulted in a concentration-dependent reversion of luciferase repression, indicating that kshv-miR-K12-3 is selectively capable of causing the named effect (Figure 4B). To test whether the predicted binding site on the LRRC8D mRNA is the true and sole site of interaction with kshv-miR-K12-3, we mutated the seed region of the putative binding site of kshv-miR-K12-3 by inserting five point mutations according to Ziegelbauer et al. (Ziegelbauer et al., 2009) (Figure S3B). When the vector carrying this mutation was cotransfected with the vector expressing the ten intronic KSHV miRNAs or miR-K12-3 alone, the miRNA effect was no longer detectable (Figure 4C). These findings demonstrate that binding of kshv-miR-K12-3 to this single site in the 3′UTR of LRRC8D transcripts is necessary and sufficient to exert the inhibitory effect.

GEMIN8 and NHP2L1 Are Both Regulated through a KSHV miRNA-Binding Site within Their Coding Regions

Two KSHV miRNA targets, GEMIN8 and NHP2L1, could not be validated by 3′UTR dual-luciferase assays. Using RNAhybrid, we tested whether they might be regulated by binding sites located within their coding sequences or 5′UTRs. We identified

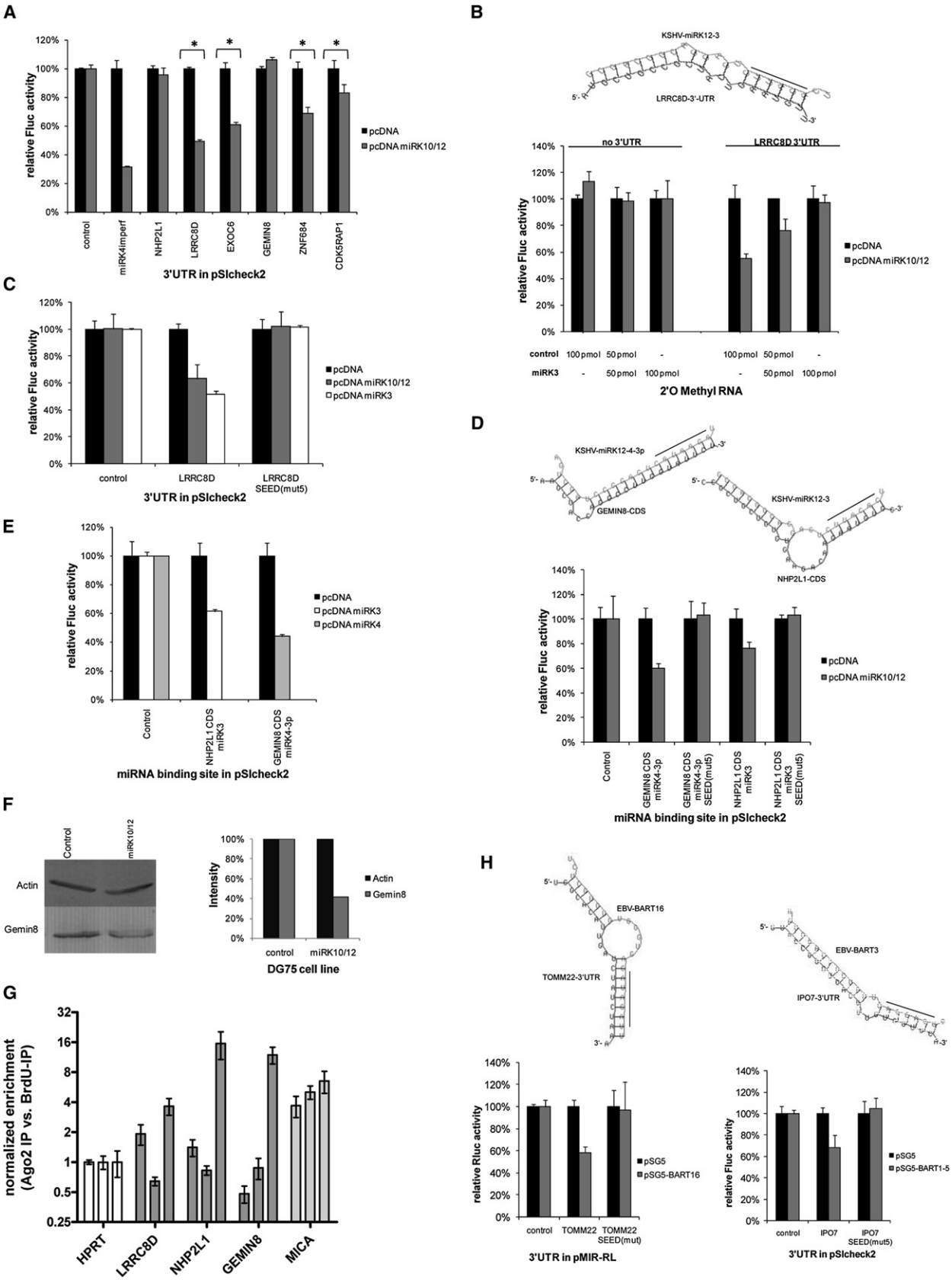
A
relative Fluc activity
pcDNA
pcDNA miRK10/12
control
miRK4Imperf
NHP2L1
LRRC8D
EXOC6
GEMIN8
ZNF684
CDK5RAP1
3'UTR in pSIcheck2
B
KSHV-miRK12-3
LRRC8D-3'-UTR
no 3'UTR
LRRC8D 3'UTR
control
miRK3
2'O Methyl RNA
C
pcDNA miRK3
control
LRRC8D
LRRC8D SEED(mut5)
3'UTR in pSIcheck2
D
KSHV-miRK12-4-3p
GEMIN8-CDS
KSHV-miRK12-3
NHP2L1-CDS
GEMIN8 CDS miRK4-3p
GEMIN8 CDS miRK4-3p SEED(mut5)
NHP2L1 CDS miRK3
NHP2L1 CDS miRK3 SEED(mut5)
miRNA binding site in pSIcheck2
E
pcDNA miRK4
Control
NHP2L1 CDS miRK3
GEMIN8 CDS miRK4-3p
miRNA binding site in pSIcheck2
F
Control
miRK10/12
Actin
Gemin8
Intensity
DG75 cell line
G
normalized enrichment (Ago2 IP vs. BrdU-IP)
HPRT
LRRC8D
NHP2L1
GEMIN8
MICA
H
EBV-BART16
TOMM22-3'UTR
EBV-BART3
IPO7-3'UTR
relative Rluc activity
pSG5
pSG5-BART16
TOMM22
TOMM22 SEED(mut)
3'UTR in pMIR-RL
pSG5-BART1-5
IPO7
IPO7 SEED(mut5)
3'UTR in pSIcheck2

a high confidence interaction site for kshv-miR-K12-4-3p in the coding sequence of GEMIN8 and for kshv-miR-K12-3 in the coding sequence of NHP2L1 (Figure 4D, Tables S6B and S6C). Reporter constructs were created containing the putative binding sites (128 nt for GEMIN8 and 146 nt for NHP2L1), and dual-luciferase assays were performed. In both cases, expression of the intronic KSHV miRNAs as well as the predicted individual KSHV miRNAs resulted in a significant repression of firefly luciferase activity, indicating that these two putative miRNA-binding sites can indeed be targeted by the respective KSHV miRNAs. In both cases, binding sites were confirmed by mutating the seed region of the predicted binding site by introducing five point mutations (Figure 4D, Figures S3B and S3C). In addition, significant repression of the luciferase signal was also observed upon cotransfection with the respective single KSHV-miRNA-expressing vectors (Figure 4E). To test whether regulation by KSHV miRNAs had any effect on endogenous protein levels, we performed quantitative Western blot analysis using antibodies to GEMIN8 and NHP2L1. While no specific signal could be obtained for NHP2L1 (data not shown), a 2.5-fold downregulation of GEMIN8 protein levels was observed for GEMIN8 in DG75-10/12 compared to DG75-eGFP (Figure 4F).

To test whether isolated expression of kshv-miR-K12-3 or -K12-4 was sufficient to efficiently recruit LRRC8D, NHP2L1, and GEMIN8 transcripts to Ago2 complexes, we performed RISC pull-downs in 293 cells expressing doxycyclin (dox)-inducible kshv-miR-K12-3 (293-miR-K3) or -K12-4 (293-miR-K4). Consistent with regulation of LRRC8D and NHP2L1 by kshv-miR-K12-3, qPCR revealed significant enrichment of their transcripts in the Ago2-IPs of 293-miR-K3 cells following dox induction, but not in 293-miR-K4 cells (Figure 4G). A weak enrichment of GEMIN8 in dox-induced 293-K12-4 cells was also detectable, but this did not quite reach significance. Therefore, additional miRNAs may be involved in recruiting NHP2L1 and GEMIN8 to Ago2 complexes.

Finally, we also cloned 3′UTRs of three putative EBV miRNA targets, namely TOMM22 (mitochondrial import receptor subunit TOM22 homolog), IPO7 (importin 7), and RAB13 (RAB13, member RAS oncogene family) into dual-luciferase vectors. Potential binding sites for EBV miRNAs were predicted using RNAhybrid (Rehmsmeier et al., 2004). In both cases, the predicted binding sites (for ebv-miR-BART-16 and ebv-miR-BART-3, respectively) were validated by luciferase assays by cotransfection of expression vectors for the respective miRNAs (Figure 4H). Mutagenesis of the seed regions of the putative binding sites resulted in complete loss of inhibition. No inhibition of luciferase expression by EBV miRNAs was detectable for the RAB13 reporter construct (data not shown).

Characteristics of Cellular and Viral miRNA Targets

It has been a long-standing matter of debate to what extent miRNAs influence the stability of their targets. Therefore, we compared transcript half-lives of the cellular miRNA targets with those of ~8300 genes expressed in BL41 taken from our recently published atlas of transcript half-lives in human B cells (Friedel et al., 2009). This atlas contained precise transcript half-lives for ~70% of the cellular miRNA targets. With a median half-life of 4.3 hr, transcript half-lives of the targets of cellular miRNAs were significantly shorter (Kolmogorov-Smirnov test, $p < 2.2 \times 10^{-16}$) than transcript half-lives of the other genes expressed in human B cells (median $t_{1/2} = 5.4$ hr) (Figure 5A). In contrast, the median half-life of transcripts identified as viral miRNA targets was not significantly shorter than the overall median RNA half-life, indicating that cellular transcripts with short half-lives are not preferentially targeted by viral miRNAs. Next, we looked at the correlation of the enrichment in the Ago2-IP in BL41

Figure 4. Validation of KSHV miRNA Targets by Dual-Luciferase Assays

Indicator vectors carrying no additional sequences, or candidate 3′UTR sequences inserted 3′ to the firefly luciferase gene, were cotransfected into HEK293 either with empty pcDNA or pcDNA expressing the ten intronic KSHV miRNAs (pcDNAmiRK10/12), kshv-miR-K12-3 (pcDNAmiRK3), or kshv-miR-K12-4 (pcDNA-miRK4). A vector containing an imperfect match for kshv-miR-K12-4 was used as positive control. Dual-luciferase assays were performed 16 hr later. Firefly to renilla luciferase ratios were normalized to the empty pSIcheck2 vector as described (Gottwein et al., 2007). All dual-luciferase experiments were performed at least three times in triplicate. Values represent the mean ± SD of representative experiments.

(A) Six candidate 3′UTRs of putative KSHV miRNA targets were tested, four of which reproducibly caused significant downregulation of firefly luciferase expression (indicated by asterisks).

(B) The interaction between kshv-miRK12-3 and the 3′UTR of LRRC8D was modeled using RNA Hybrid (Rehmsmeier et al., 2004) (top). The black line indicates the seed region of kshv-miR-K12-3. Luciferase derepression analysis of LRRC8D 3′UTR with a sequence-specific AntagomiR (2′O-methyl RNA) demonstrated a concentration-dependent derepression indicating that LRRC8D is indeed targeted by kshv-miR-K12-3 (bottom).

(C) KSHV miRNA mediated repression of luciferase activity via the LRRC8D 3′UTR after coexpression of the ten intronic KSHV miRNAs or miR-K12-3 alone was lost upon deletion of the putative SEED match for kshv-miR-K12-3.

(D) Putative target sites for KSHV miRNAs located in the coding sequence of GEMIN8 and NHP2L1 (top) were cloned into pSIcheck2 in the 3′UTR of the firefly luciferase gene. Repression of firefly luciferase activity occurred when KSHV miRNAs were cotransfected. This effect was abolished by the introduction of five point mutations into the putative SEED-matching regions (bottom).

(E) The sensor vectors carrying putative miRNA target sites from the coding sequence of NHP2L1 and GEMIN8 were cotransfected with the respective individual constructs expressing miR-K12-3 or miR-K12-4 resulting in significant repression of luciferase activity.

(F) Proteins were labeled by using Alexa488-conjugated secondary antibodies and scanned in the Fluoimager. Reduction of GEMIN8 level was quantified by employing the AIDA software.

(G) RISC-IPs were performed from 293 cells expressing either kshv-miR-K12-3 (293-miR-K3) or -miR-K12-4 (293-miR-K4) following induction with doxycyclin. BCBL-1 served as control. For each gene, mRNA enrichment (qPCR of Ago2-IP versus control-IP) normalized for HPRT expression levels is shown for 293-miR-K3 (left), 293-miR-K4 (middle), and BCBL-1 (right). Enrichment of LRRC8D ($p = 0.011$) and NHP2L1 ($p = 0.037$) was significant in 293-miR-K3 compared with 293-miR-K4 (unpaired t test). Enrichment of GEMIN8 did not quite reach significance ($p = 0.062$). Means ± SDs represent combined data from three independent RISC-IPs per condition.

(H) Binding sites for ebv-miR-BART16 and ebv-miR-BART3 in the 3′UTR of TOMM22 and IPO7, respectively, are shown (top). Luciferase assays with sensor vectors carrying the 3′UTRs of TOMM22 and IPO7 demonstrated significant repression by ebv-miR-BART16 and ebv-miR-BART3, respectively. These effects were completely reversed when the seed regions of the predicted binding sites (RNAhybrid) were mutated (bottom).

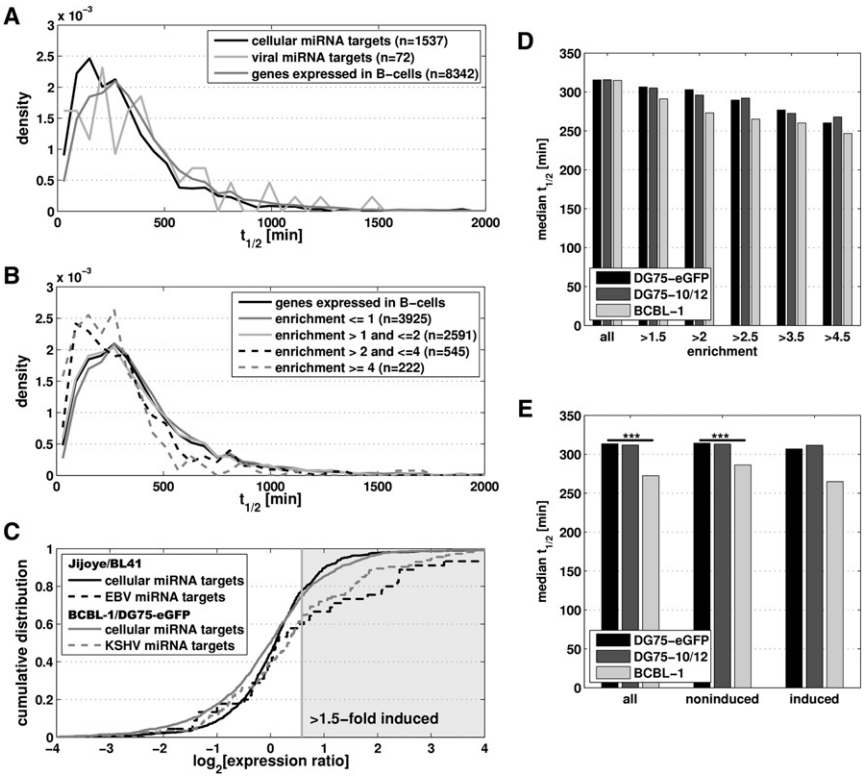

Figure 5. Effect of miRNAs on Target RNA Stability

(A) Distribution of the transcript half-life of the targets of cellular and viral miRNAs was compared with the transcript half-life of all genes for which RNA half-lives were available from our recently published atlas of RNA half-lives in human B cells (BL41; n = 8,342). The density distribution was estimated by binning genes according to transcript half-lives in intervals of 60 min, counting the number of genes in each bin, and then normalizing the counts such that the area under the curve is 1. Transcript half-life (*x* axis) is plotted against the estimated density (*y* axis). RNA half-lives of cellular miRNA targets were significantly lower (Kolmogorov-Smirnov test, $p < 2.2 \times 10^{-16}$) than for all other cellular transcripts expressed in human B cells for which RNA half-lives were available (Friedel et al., 2009). For viral miRNA targets, no significant difference was observed. Please note that no viral miRNAs are expressed in BL41 for which the RNA half-lives were obtained.

(B) The extent of recruitment to Ago2 complexes (enrichment in the Ago2-IP) negatively correlated with transcript half-life. The distribution of the half-life of transcripts enriched either ≥ 4-fold, 2- to 4-fold, 1- to 2-fold, and less than 1-fold as well as of all 8342 cellular transcripts was compared. A highly significant, negative correlation in between transcript half-life and recruitment to Ago2 complexes was observed (Spearman correlation coefficient, −0.13; p value $< 10^{-16}$).

(C) Effect of viral miRNAs on target mRNA levels. The cumulative distribution of alterations in expression levels of cellular, KSHV, and EBV miRNA targets represented either by the BrdU-IP (for DG75-eGFP versus BCBL-1) or total RNA (for BL41 versus Jijoye) is shown. Genes induced either in BCBL-1 or Jijoye are represented by a $\log_2$ expression ratio > 1.0; genes downregulated in these cells compared to either DG75-eGFP or BL41 by a ratio < 1.0. Genes induced > 1.5-fold in infected cells (right of gray vertical line) are provided in Tables S4C and S4D.

(D) Correlation of enrichment in the Ago2-IP with transcript half-life. The median half-life of transcripts which were enriched more than the indicated value in the Ago2-RIP-Chip in each of the indicated cell lines (DG75-eGFP, DG75-10/12, and BCBL-1) are shown.

(E) KSHV miRNAs destabilize their targets. RNA half-lives of the KSHV miRNA targets identified by Ago2-RIP-Chip were determined in DG75-eGFP, DG75-10/12, and BCBL-1 based on nascent / total RNA ratios (n = 3; for details, see Table S7B). Their RNA half-lives were significantly shorter in BCBL-1 (Friedman test, $p = 6.74 \times 10^{-6}$) than in both DG75-eGFP and DG75-10/12. This was seen for both the induced and noninduced KSHV miRNA targets but was only significant for the noninduced ($p = 5.25 \times 10^{-6}$), presumably due to the smaller number of induced (n = 35) versus noninduced (n = 70) KSHV miRNA targets for which RNA half-lives could be determined.

with transcript half-life (Figure 5B). We observed a small but highly significant negative correlation in between transcript half-life and recruitment to Ago2 complexes (Spearman correlation coefficient, −0.13; p value $< 10^{-16}$). Thus, these data support previous studies demonstrating that cellular miRNAs have a small but measurable impact on target RNA stability (Baek et al., 2008; Selbach et al., 2008). Our data now extend these findings, showing that the effect on RNA stability correlates with the extent of target recruitment to Ago2 complexes.

To investigate the effect of viral miRNAs on the transcript levels of their targets, we first compared expression levels in DG75-eGFP and BCBL-1 (for KSHV miRNA targets) as well as in BL41 and Jijoye (for EBV miRNA targets). As a reference, the changes in expression levels of the 2337 targets of the cellular miRNAs were used (Figure 5C). For both KSHV and EBV miRNA targets, the extent and distribution of downregulation was very similar to that observed for the cellular miRNA targets. Interestingly, we noted that a substantial number of both KSHV and EBV miRNA targets were expressed at higher levels in BCBL-1 and Jijoye, respectively. In order to assess whether KSHV miRNAs preferentially target transcripts transcribed at higher rates in infected than in uninfected B cells or whether they are directly responsible for the increased total RNA levels by enhancing RNA stability, we determined RNA half-lives for DG75-eGFP, DG75-10/12, and BCBL-1 by metabolic tagging of nascent RNA with 4-thiouridine (Friedel et al., 2009). Following separation of total RNA into nascent and untagged pre-existing RNA, three biological replicates of all three RNA fractions were analyzed on Affymetrix Gene ST 1.0 arrays. RNA half-lives of cellular and viral miRNA targets are provided in Tables S7A and S7B, respectively. Again, we observed a significant, linear correlation of recruitment of transcripts to Ago2 complexes with RNA half-life for all three cell lines (Figure 5D). In DG75-eGFP and DG75-10/12, half-life distribution and median RNA half-life of all KSHV miRNA targets were indistinguishable from other cellular transcripts. In contrast, RNA half-life of KSHV miRNA targets was significantly shorter in BCBL-1 ($t_{1/2m}$ = 272 min, Friedman test $p = 6.74 \times 10^{-6}$) than in both DG75-eGFP ($t_{1/2m}$ = 314 min) and DG75-10/12 ($t_{1/2m}$ = 312 min, Figure 5E). These data are consistent with the substantially greater mean

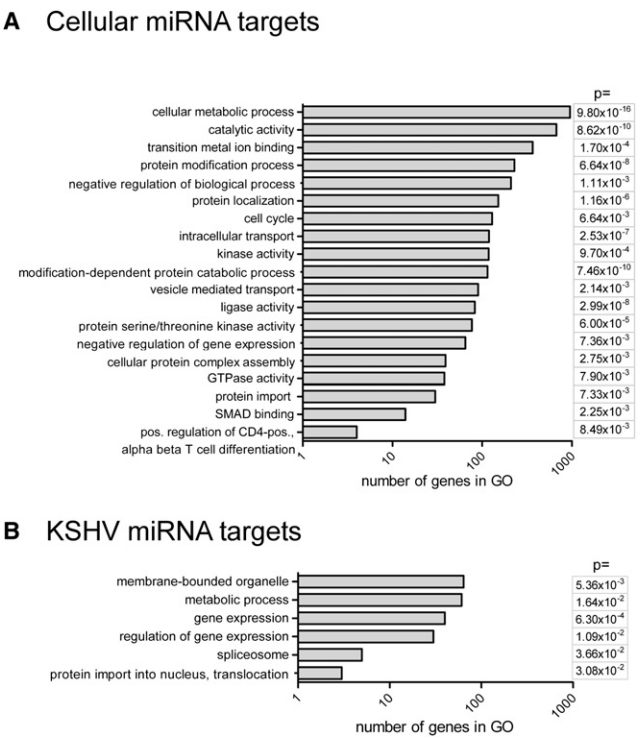

Figure 6. Transcripts Targeted by miRNAs Are Enriched for GO-Annotated Functional Classes

Selected GO functional classes of transcripts targeted by cellular (A) or KSHV (B) miRNAs are shown. The number of transcripts in each class is indicated on a logarithmic scale, along with the respective p value.

enrichment of the 114 KSHV miRNA targets in the Ago2-IP of BCBL-1 (~5.5-fold) than of DG75-10/12 (~1.5-fold) and DG75-eGFP (~1.2-fold). The half-lives of induced and noninduced target transcripts were very similar in BCBL-1, indicating that the increased levels of miRNA target transcripts in BCBL-1 are not due to enhanced RNA stability but rather an increase in transcriptional rate that is counteracted by the viral miRNAs.

To identify functional categories enriched among both cellular and viral miRNA targets, we performed a Gene Ontology (GO) overrepresentation analysis. For targets of cellular miRNAs, a large number of GO terms were significantly overrepresented, consistent with cellular miRNAs being involved in a broad spectrum of cellular processes (Table S8A). A selected list of these is shown in Figure 6A. KSHV miRNA targets were preferentially involved in gene expression and its regulation as well as the spliceosome and protein import into the nucleus (Figure 6B, Table S8B). No functional categories were overrepresented among the EBV miRNA targets (Table S8C).

DISCUSSION

Since the identification of virally encoded miRNAs, research on them has been hampered by the lack of high-confidence targets. Here we provide a large number of such targets for the two human γ-herpesviruses, KSHV (n = 114) and EBV (n = 44), as well as cellular miRNAs (n = 2337). Predicted miRNA-binding sites of cellular miRNAs were highly overrepresented in coding sequences ($p = 2.02 \times 10^{-27}$) and 3′UTRs ($p = 6.19 \times 10^{-63}$), but not in 5′UTRs ($p = 8.59 \times 10^{-3}$). For the viral miRNA targets we identified, predicted binding sites were predominantly overrepresented in target 3′UTRs. We used dual-luciferase assays to validate six KSHV miRNA targets. For four of them we observed significant regulation by KSHV miRNAs via their 3′UTRs. The two remaining genes (GEMIN8 and NHP2L1) are regulated by binding sites located within their coding regions. For GEMIN8 this resulted in a significant reduction of protein levels.

Despite the much larger number of EBV miRNAs potentially being responsible for regulation of transcripts selectively enriched in EBV-infected cells, we could validate TOMM22 and IPO7 as targets of ebv-miR-BART16 and ebv-miR-BART3, respectively. These two proteins are involved in import of proteins from the cytosol into the mitochondria (TOMM22) (Saeki et al., 2000; Yano et al., 2000) and the nucleus (IPO7) (Gorlich et al., 1997). Antisense knockdown of TOMM22 has been shown to inhibit the association of the proapoptotic protein BAX with mitochondria and thus prevent BAX-induced apoptosis (Bellot et al., 2007). Recently, IPO7 has also been implicated in innate immunity. Antisense knockdown of IPO7 in macrophages resulted in reduced production of the proinflammatory cytokine IL-6 upon LPS challenge (Yang et al., 2009a). This study also identified FBXO9 as one of four factors required for efficient production of IL-6 in J774A.1 macrophages. While the function of FBXO9 is unknown, it is possible to be involved in phosphorylation-dependent ubiquitination of IκB or another important signaling molecule in the TLR4 pathway or another pathway that is activated in response to LPS (Yang et al., 2009a). Interestingly, FBXO9 is also in our list of 44 EBV miRNA targets and was validated by qPCR. Thus, it is intriguing to speculate that EBV taps the proinflammatory signaling networks by recruitment of both IPO7 and FBXO9 transcripts to Ago2 complexes. In summary, this is indicative of EBV miRNAs modulating cellular trafficking and protein localization to counteract innate immunity and apoptosis.

In the last few years a number of transcripts have been identified to be targeted by KSHV and EBV miRNAs. The majority of KSHV targets were identified based on the finding that KSHV encodes an ortholog of hsa-miR-155 (kshv-miR-K12-11) (Gottwein et al., 2007; Skalsky et al., 2007). Gottwein et al. identified 12 genes to be targeted by both kshv-miR-K12-11 and hsa-miR-155. We found 3 of 12 (25%) of these genes to be enriched > 2-fold in BCBL-1, but not in DG75-eGFP or BL41. Of these, SLA (Src-like-adaptor, transcript variant 1) was the most strongly enriched transcript in BCBL-1 (18.3-fold). Interestingly, it appeared to be induced > 4-fold in BCBL-1. An additional 4 of 12 genes (33%) were enriched > 1.5-fold in BCBL-1. Finally, 5 genes (42%) were enriched > 1.5-fold stronger in Jijoye or BL41 B95.8 than in both control cell lines, consistent with their regulation by hsa-miR-155 induced upon EBV infection (Gatto et al., 2008). In summary, only 1 of the 12 genes (BCLAF1) was not enriched > 1.5-fold in BCBL-1, BL41 B95.8, or Jijoye. We could confirm the differential regulation of MICA and MICB by both KSHV and EBV as well as cellular miRNAs (Stern-Ginossar et al., 2007, 2008). During the revision of this paper, Lei et al. identified kshv-miR-K12-1 to target the NFκB inhibitor IκBα (NFKBIA) via two binding sites in its 3′UTR

(Lei et al., 2010). By reducing IκBα protein levels the NFκB pathway is activated, mediating vFLIP inhibition of KSHV lytic replication (Ye et al., 2008). Our data nicely confirm this regulation by revealing a selective 7.3-fold enrichment of NFKBIA transcripts in the Ago2-IP of BCBL-1 and to a lesser extent (2.5-fold) in DG75-10/12. In total, about 60% of the known KSHV and EBV miRNA targets showed detectable enrichment in our assay (summarized in Table S3B). The analysis of other published miRNA targets exemplifies an important aspect of using RIP-Chip to identify miRNA targets. In contrast to other methods, this approach is based on positive selection of viral miRNA targets. In consequence, a lack of enrichment does not exclude a transcript to be targeted by miRNAs due to the following reasons: First, some of the transcripts may be expressed at very low levels and thus be below the detection limit of the microarrays. Second, an enrichment of as little as 1.2-fold still resulted in a highly significant overrepresentation of predicted miRNA-binding sites for cellular miRNA targets ($p < 10^{-62}$). Thus, it may still be consistent with regulation by a viral miRNA. As we restricted our analysis to strongly enriched targets (>3-fold), we excluded a large number of viral miRNA targets. Finally, expression levels of both miRNA and its targets define whether a miRNA is able to exert a significant effect. Expression of both is influenced by the cell line and assay employed; e.g., luciferase assays in HEK293 cells with transfected miRNA expression vectors and reporter constructs.

We observed a significantly overrepresented number of KSHV and EBV miRNA targets to be expressed at higher levels in BCBL-1 and Jijoye, respectively, than in the uninfected cells. By measuring RNA half-lives in DG75-eGFP, DG75-10/12, and BCBL-1 using a new approach we recently developed (Dölken et al., 2008; Friedel et al., 2009), we found that, despite higher total RNA levels, the RNA half-life of the induced KSHV miRNA targets was significantly shorter in BCBL-1 than in DG75-10/12, DG75-eGFP, and BL41. We conclude that KSHV miRNAs counteract the increased transcription rates of these genes in the infected cells and hypothesize that KSHV (and also EBV) miRNAs preferentially target transcripts induced in the infected cells.

Another important finding of our study is the linear correlation between recruitment of transcripts to Ago2-complexes, i.e., enrichment in the Ago2-IP, and transcript half-life. This indicates that this approach allows a quantitative estimate on the true extent of miRNA mediated regulation. It is tempting to speculate that more strongly regulated targets are more likely to be biologically relevant. Therefore, this approach may help to decide which of the large number of viral miRNA targets to pursue in further studies. This concept is supported by the strong enrichment we observed for both MICB and NFKBIA, both of which were not only confirmed by luciferase assay but were also shown to exert a significant biological effect upon downregulation. In this respect, we provide a large number of high-confidence viral miRNA targets. In addition, we provide data for numerous other transcripts predominantly enriched in either BCBL-1 or Jijoye that did not quite fulfill our stringent criteria but which most likely are also targeted by the viral miRNAs. Thus, these data provide an important basis for further studies aimed to characterize the viral miRNA targets relevant for the interaction of the virus with its human host.

EXPERIMENTAL PROCEDURES

Generation of Cell Lines Expressing KSHV miRNAs

Human B cells (DG75-eGFP and DG75-10/12) stably expressing either eGFP or the ten intronic KSHV miRNAs were generated using the "Virapower" lentiviral transduction system (Invitrogen) and recombinational cloning following the manufacturer's instructions. HEK293 cell lines expressing either doxycyclin-inducible kshv-miR-K12-3 or -K12-4 (293-K3 and 293-K4) were generated using the Flp-In T-REx-293 cell line (Invitrogen) according to the manufacturer's instructions. To induce KSHV miRNA expression, 1 μg/mL doxycycline was added for 48 hr.

Immunoprecipitation of Human Argonaute 2 Complexes

For the RISC-IPs of human B cells, 5×10^8 cells were taken for each replicate and washed twice in PBS before lysis in 10 ml lysis buffer containing 25 mM Tris HCl (pH 7.5), 150 mM KCl, 2 mM EDTA, 0.5% NP-40, 0.5 mM DTT, and protease inhibitor Complete (Roche). DTT and protease inhibitors were always prepared freshly and added immediately before use. Lysates were incubated for 30 min at 4°C and cleared by centrifugation at 20,000 g for 30 min at 4°C. Total RNA was prepared from 100 μl of cell lysates using the miRNeasy kit (QIAGEN) following the manufacturer's instructions. RISC-IPs were performed with a few modifications to the previously described protocol (Beitzinger et al., 2007). In short, 6 μg of purified monoclonal hAgo2 antibody (α-hAgo2; 11A9) or monoclonal BrdU-antibody (Abcam; used as control) was added to 5 ml of RPMI medium and incubated with 60 μl of protein G Sepharose beads (GE Healthcare) in Pierce centrifuge columns (Thermo Scientific) under constant rotation at 4°C overnight. Columns were drained by gravity flow and washed once with the lysis buffer. Beads were subsequently incubated with 5 ml of cell lysates for 2.5 hr under constant rotation at 4°C. After incubation, the beads were washed four times with IP wash buffer (300 mM NaCl, 50 mM Tris HCl [pH 7.5], 5 mM $MgCl_2$, 0.1% NP-40, 1 mM NaF) and once with PBS to remove residual detergents. RNA was recovered from the beads by adding 700 μl of Qiazol to the columns. After 5 min, the Qiazol lysates were collected from the columns. This step was repeated once, and the Qiazol lysates were combined. RNA was prepared using the miRNeasy kit (QIAGEN) according to the manufacturer's instructions. RNA samples were eluted in 30 μl H_2O. For RISC-IPs from 293 cells (expressing single KSHV-miRNAs upon 48 hr induction by doxycyclin), lysates prepared from a single 15 cm dish (~80% confluent) were used, and the IP assay was scaled down by 2-fold. Lysates from BCBL-1 served as control.

Microarray Sample Labeling, Hybridization, and Preprocessing

For the microarray analysis, 200 ng RNA of each sample was amplified and labeled using the Affymetrix Whole-Transcript (WT) Sense Target Labeling Protocol without rRNA reduction. Affymetrix GeneChip Human Gene 1.0 ST arrays were hybridized, washed, stained, and scanned according to the protocol described in WT Sense Target Labeling Assay Manual. Microarray data were assessed for quality and normalized with RMA. All microarray data are available at Gene Expression Omnibus (GEO) at http://www.ncbi.nlm.nih.gov/geo/query/acc.cgi?token=lnelhkuucokacjo&acc=GSE17180.

cDNA Synthesis and Quantitative Real-Time PCR

3′-polyadenylation and cDNA synthesis were performed for Ago2-IP, BrdU-IP, and total RNA samples in a single-step reaction using the miScript Reverse Transcription kit (QIAGEN). The efficiency of every RISC-IP was monitored by Light Cycler qRT-PCR for cellular miRNA Let7a using the let7a-specific primer 5′-TGAGGTAGTAGGTTGTATAGTT-3′. Microarray data of 24 transcripts were validated by TaqMan PCR using the ABI Prism 7000 sequence detection system (Applied Biosystems). TaqMan probes were taken from the Universal Probe Library (Roche), and selection of probe-primer combinations was performed using the Assay Design Centre (Roche, http://www.universalprobelibrary.com). A list of the utilized PCR primers and probes is provided in Table S9.

Luciferase Repression and 2′O-Methyl-RNA Derepression Assay

To analyze 3′UTRs of genes of interest in terms of their ability to interact with miRNAs, we generated the vector pSIcheck-XE-DEST-sense (reporter plasmid, see Table S9 for details). For 6 of the 11 KSHV miRNA targets

confirmed by quantitative PCR, we were able to amplify their full-length 3′UTRs by PCR using DNA prepared from DG75. To validate putative EBV miRNA targets, we amplified the full-length 3′UTRs of TOMM22, IPO7, and RAB13 by PCR. TOMM22 and RAB13 were inserted into pMIR-RL (Zhu et al., 2009) by conventional cloning, and IPO7 was inserted into pSIcheck-XE-DEST by recombinatorial cloning. For dual-luciferase assays, 10 ng of the reporter plasmid was cotransfected into HEK293 cells in 24-well plates with either the respective miRNA-expressing pcDNA vector (200 ng) or the empty pcDNA vector as negative control. Transfection was carried out using FuGene 6 (Roche) according to the manufacturer's instructions. Sixteen hours after transfection, luciferase activity was measured employing the Dual-Luciferase Reporter Assay (Promega) and the luminometer Fluostar Optima (BMG-Labtech) as recommended by the manufacturers. For derepression analysis, HEK293 cells were seeded on 24-well plates as for the luciferase repression assay and transfected with 100 pmol 2′O-methyl-RNA using Lipofectamine 2000 (Invitrogen). Six hours after transfection, the medium was changed and reporter and miRNA expression plasmids were cotransfected. Sixteen hours later, luciferase activity was measured.

Overrepresentation of Predicted miRNA-Binding Sites

Cellular miRNAs expressed in all six cell lines were obtained from the miRNA expression atlas (Landgraf et al., 2007). Their sequences as well as the sequences of the KSHV and EBV miRNAs were obtained from miRBase v.12 (http://microrna.sanger.ac.uk/sequences/). The 3′UTRs, coding sequences, and 5′UTRs for all cellular genes were downloaded from Ensembl (http://www.ensembl.org/). For all of these, miRNA target sites were predicted using PITA (Kertesz et al., 2007). Overrepresentation was determined using Fisher's exact test.

Metabolic Tagging of Nascent RNA Using 4-Thiouridine

Nascent RNA was tagged in DG75-eGFP, DG75-10/12, and BCBL-1 for 1 hr by adding 100 μM 4-thiouridine (4sU) to cell culture medium. Biotinylation of 4sU-tagged RNA and separation of total RNA into nascent and untagged pre-existing RNA were performed as described (Dölken et al., 2008; Friedel et al., 2009). RNA half-lives were determined based on nascent/total RNA ratios. Median RNA half-life was normalized to 315 min as obtained for BL41.

Further experimental details are provided in the Supplemental Experimental Procedures.

SUPPLEMENTAL INFORMATION

Supplemental Information includes three figures, Supplemental Experimental Procedures, and nine tables and can be found with this article at doi:10.1016/j.chom.2010.03.008.

ACKNOWLEDGMENTS

We would like to thank Bernd Rädle and Silvia Weide for their excellent technical assistance. This work was supported by the German Bundesministerium fuer Bildung und Forschung (NGFN-Plus #01GS0801/3/4 to L.D., U.H.K., J.H., F.G., F.E., C.C.F., and R.Z.), MRC (G0501453 to J.H.), Friedrich-Baur Stiftung (to L.D.), CNRS ATIP starting grant and Ligue Contre le Cancer (to S.P.), the Deutsche Forschungsgemeinschaft (FO855 to G.M. and SFB 576 to J.H.), the Max-Planck-Society (to G.M.), and the Bayerisches Staatsministerium für Wissenschaft, Forschung und Kunst (BayGene to J.H.).

Received: August 27, 2009
Revised: November 25, 2009
Accepted: March 20, 2010
Published: April 21, 2010

REFERENCES

Baek, D., Villen, J., Shin, C., Camargo, F.D., Gygi, S.P., and Bartel, D.P. (2008). The impact of microRNAs on protein output. Nature *455*, 64–71.

Bandi, N., Zbinden, S., Gugger, M., Arnold, M., Kocher, V., Hasan, L., Kappeler, A., Brunner, T., and Vassella, E. (2009). miR-15a and miR-16 are implicated in cell cycle regulation in a Rb-dependent manner and are frequently deleted or down-regulated in non-small cell lung cancer. Cancer Res. *69*, 5553–5559.

Baroni, T.E., Chittur, S.V., George, A.D., and Tenenbaum, S.A. (2008). Advances in RIP-chip analysis: RNA-binding protein immunoprecipitation-microarray profiling. Methods Mol. Biol. *419*, 93–108.

Barozzi, P., Potenza, L., Riva, G., Vallerini, D., Quadrelli, C., Bosco, R., Forghieri, F., Torelli, G., and Luppi, M. (2007). B cells and herpesviruses: a model of lymphoproliferation. Autoimmun. Rev. *7*, 132–136.

Beitzinger, M., Peters, L., Zhu, J.Y., Kremmer, E., and Meister, G. (2007). Identification of human microRNA targets from isolated argonaute protein complexes. RNA Biol. *4*, 76–84.

Bellot, G., Cartron, P.F., Er, E., Oliver, L., Juin, P., Armstrong, L.C., Bornstein, P., Mihara, K., Manon, S., and Vallette, F.M. (2007). TOM22, a core component of the mitochondria outer membrane protein translocation pore, is a mitochondrial receptor for the proapoptotic protein Bax. Cell Death Differ. *14*, 785–794.

Cai, X., Lu, S., Zhang, Z., Gonzalez, C.M., Damania, B., and Cullen, B.R. (2005). Kaposi's sarcoma-associated herpesvirus expresses an array of viral microRNAs in latently infected cells. Proc. Natl. Acad. Sci. USA *102*, 5570–5575.

Cai, X., Schafer, A., Lu, S., Bilello, J.P., Desrosiers, R.C., Edwards, R., Raab-Traub, N., and Cullen, B.R. (2006). Epstein-Barr virus microRNAs are evolutionarily conserved and differentially expressed. PLoS Pathog. *2*, e23. 10.1371/journal.ppat.0020023.

Carbone, A., Gloghini, A., Vaccher, E., Zagonel, V., Pastore, C., Dalla, P.P., Branz, F., Saglio, G., Volpe, R., Tirelli, U., and Gaidano, G. (1996). Kaposi's sarcoma-associated herpesvirus DNA sequences in AIDS-related and AIDS-unrelated lymphomatous effusions. Br. J. Haematol. *94*, 533–543.

Carbone, A., Gloghini, A., and Dotti, G. (2008). EBV-associated lymphoproliferative disorders: classification and treatment. Oncologist *13*, 577–585.

Choy, E.Y., Siu, K.L., Kok, K.H., Lung, R.W., Tsang, C.M., To, K.F., Kwong, D.L., Tsao, S.W., and Jin, D.Y. (2008). An Epstein-Barr virus-encoded microRNA targets PUMA to promote host cell survival. J. Exp. Med. *205*, 2551–2560.

Delecluse, H.J., Feederle, R., O'Sullivan, B., and Taniere, P. (2007). Epstein Barr virus-associated tumours: an update for the attention of the working pathologist. J. Clin. Pathol. *60*, 1358–1364.

Dölken, L., Ruzsics, Z., Radle, B., Friedel, C.C., Zimmer, R., Mages, J., Hoffmann, R., Dickinson, P., Forster, T., Ghazal, P., and Koszinowski, U.H. (2008). High-resolution gene expression profiling for simultaneous kinetic parameter analysis of RNA synthesis and decay. RNA *14*, 1959–1972.

Dourmishev, L.A., Dourmishev, A.L., Palmeri, D., Schwartz, R.A., and Lukac, D.M. (2003). Molecular genetics of Kaposi's sarcoma-associated herpesvirus (human herpesvirus-8) epidemiology and pathogenesis. Microbiol. Mol. Biol. Rev. *67*, 175–212.

Easow, G., Teleman, A.A., and Cohen, S.M. (2007). Isolation of microRNA targets by miRNP immunopurification. RNA *13*, 1198–1204.

Friedel, C.C., Dölken, L., Ruzsics, Z., Koszinowski, H., and Zimmer, R. (2009). Conserved principles of mammalian transcriptional regulation revealed by RNA half-life. Nucleic Acids Res. *37*, e115.

Fu, L.Y., Jia, H.L., Dong, Q.Z., Wu, J.C., Zhao, Y., Zhou, H.J., Ren, N., Ye, Q.H., and Qin, L.X. (2009). Suitable reference genes for real-time PCR in human HBV-related hepatocellular carcinoma with different clinical prognoses. BMC Cancer *9*, 49.

Gaidano, G., Gloghini, A., Gattei, V., Rossi, M.F., Cilia, A.M., Godeas, C., Degan, M., Perin, T., Canzonieri, V., Aldinucci, D., et al. (1997). Association of Kaposi's sarcoma-associated herpesvirus-positive primary effusion lymphoma with expression of the CD138/syndecan-1 antigen. Blood *90*, 4894–4900.

Gatto, G., Rossi, A., Rossi, D., Kroening, S., Bonatti, S., and Mallardo, M. (2008). Epstein-Barr virus latent membrane protein 1 trans-activates miR-155 transcription through the NF-kappaB pathway. Nucleic Acids Res. *36*, 6608–6619.

Gorlich, D., Dabrowski, M., Bischoff, F.R., Kutay, U., Bork, P., Hartmann, E., Prehn, S., and Izaurralde, E. (1997). A novel class of RanGTP binding proteins. J. Cell Biol. *138*, 65–80.

Gottwein, E., Mukherjee, N., Sachse, C., Frenzel, C., Majoros, W.H., Chi, J.T., Braich, R., Manoharan, M., Soutschek, J., Ohler, U., and Cullen, B.R. (2007). A viral microRNA functions as an orthologue of cellular miR-155. Nature *450*, 1096–1099.

Grundhoff, A., Sullivan, C.S., and Ganem, D. (2006). A combined computational and microarray-based approach identifies novel microRNAs encoded by human gamma-herpesviruses. RNA *12*, 733–750.

Hendrickson, D.G., Hogan, D.J., Herschlag, D., Ferrell, J.E., and Brown, P.O. (2008). Systematic identification of mRNAs recruited to argonaute 2 by specific microRNAs and corresponding changes in transcript abundance. PLoS ONE *3*, e2126. 10.1371/journal.pone.0002126.

Karginov, F.V., Conaco, C., Xuan, Z., Schmidt, B.H., Parker, J.S., Mandel, G., and Hannon, G.J. (2007). A biochemical approach to identifying microRNA targets. Proc. Natl. Acad. Sci. USA *104*, 19291–19296.

Keene, J.D., Komisarow, J.M., and Friedersdorf, M.B. (2006). RIP-Chip: the isolation and identification of mRNAs, microRNAs and protein components of ribonucleoprotein complexes from cell extracts. Nat. Protoc. *1*, 302–307.

Kertesz, M., Iovino, N., Unnerstall, U., Gaul, U., and Segal, E. (2007). The role of site accessibility in microRNA target recognition. Nat. Genet. *39*, 1278–1284.

Landgraf, P., Rusu, M., Sheridan, R., Sewer, A., Iovino, N., Aravin, A., Pfeffer, S., Rice, A., Kamphorst, A.O., Landthaler, M., et al. (2007). A mammalian microRNA expression atlas based on small RNA library sequencing. Cell *129*, 1401–1414.

Lei, X., Bai, Z., Ye, F., Xie, J., Kim, C.G., Huang, Y., and Gao, S.J. (2010). Regulation of NF-kappaB inhibitor IkappaBalpha and viral replication by a KSHV microRNA. Nat. Cell Biol. *12*, 193–199.

Liu, Q., Fu, H., Sun, F., Zhang, H., Tie, Y., Zhu, J., Xing, R., Sun, Z., and Zheng, X. (2008). miR-16 family induces cell cycle arrest by regulating multiple cell cycle genes. Nucleic Acids Res. *36*, 5391–5404.

Marshall, V., Parks, T., Bagni, R., Wang, C.D., Samols, M.A., Hu, J., Wyvil, K.M., Aleman, K., Little, R.F., Yarchoan, R., et al. (2007). Conservation of virally encoded microRNAs in Kaposi sarcoma-associated herpesvirus in primary effusion lymphoma cell lines and in patients with Kaposi sarcoma or multicentric Castleman disease. J. Infect. Dis. *195*, 645–659.

Mrazek, J., Kreutmayer, S.B., Grasser, F.A., Polacek, N., and Huttenhofer, A. (2007). Subtractive hybridization identifies novel differentially expressed ncRNA species in EBV-infected human B cells. Nucleic Acids Res. *35*, e73.

Nachmani, D., Stern-Ginossar, N., Sarid, R., and Mandelboim, O. (2009). Diverse herpesvirus microRNAs target the stress-induced immune ligand MICB to escape recognition by natural killer cells. Cell Host Microbe *5*, 376–385.

Nador, R.G., Cesarman, E., Chadburn, A., Dawson, D.B., Ansari, M.Q., Sald, J., and Knowles, D.M. (1996). Primary effusion lymphoma: a distinct clinicopathologic entity associated with the Kaposi's sarcoma-associated herpes virus. Blood *88*, 645–656.

Pauley, K.M., Satoh, M., Chan, A.L., Bubb, M.R., Reeves, W.H., and Chan, E.K. (2008). Upregulated miR-146a expression in peripheral blood mononuclear cells from rheumatoid arthritis patients. Arthritis Res. Ther. *10*, R101.

Pfeffer, S., Zavolan, M., Grasser, F.A., Chien, M., Russo, J.J., Ju, J., John, B., Enright, A.J., Marks, D., Sander, C., and Tuschl, T. (2004). Identification of virus-encoded microRNAs. Science *304*, 734–736.

Pfeffer, S., Sewer, A., Lagos-Quintana, M., Sheridan, R., Sander, C., Grasser, F.A., van Dyk, L.F., Ho, C.K., Shuman, S., Chien, M., et al. (2005). Identification of microRNAs of the herpesvirus family. Nat. Methods *2*, 269–276.

Rehmsmeier, M., Steffen, P., Hochsmann, M., and Giegerich, R. (2004). Fast and effective prediction of microRNA/target duplexes. RNA *10*, 1507–1517.

Renne, R., Zhong, W., Herndier, B., McGrath, M., Abbey, N., Kedes, D., and Ganem, D. (1996). Lytic growth of Kaposi's sarcoma-associated herpesvirus (human herpesvirus 8) in culture. Nat. Med. *2*, 342–346.

Rudel, S., Flatley, A., Weinmann, L., Kremmer, E., and Meister, G. (2008). A multifunctional human Argonaute2-specific monoclonal antibody. RNA *14*, 1244–1253.

Saeki, K., Suzuki, H., Tsuneoka, M., Maeda, M., Iwamoto, R., Hasuwa, H., Shida, S., Takahashi, T., Sakaguchi, M., Endo, T., et al. (2000). Identification of mammalian TOM22 as a subunit of the preprotein translocase of the mitochondrial outer membrane. J. Biol. Chem. *275*, 31996–32002.

Samols, M.A., Hu, J., Skalsky, R.L., and Renne, R. (2005). Cloning and identification of a microRNA cluster within the latency-associated region of Kaposi's sarcoma-associated herpesvirus. J. Virol. *79*, 9301–9305.

Samols, M.A., Skalsky, R.L., Maldonado, A.M., Riva, A., Lopez, M.C., Baker, H.V., and Renne, R. (2007). Identification of cellular genes targeted by KSHV-encoded microRNAs. PLoS Pathog. *3*, e65. 10.1371/journal.ppat.0030065.

Schulz, T.F. (2006). The pleiotropic effects of Kaposi's sarcoma herpesvirus. J. Pathol. *208*, 187–198.

Selbach, M., Schwanhausser, B., Thierfelder, N., Fang, Z., Khanin, R., and Rajewsky, N. (2008). Widespread changes in protein synthesis induced by microRNAs. Nature *455*, 58–63.

Skalsky, R.L., Samols, M.A., Plaisance, K.B., Boss, I.W., Riva, A., Lopez, M.C., Baker, H.V., and Renne, R. (2007). Kaposi's sarcoma-associated herpesvirus encodes an ortholog of miR-155. J. Virol. *81*, 12836–12845.

Stern-Ginossar, N., Elefant, N., Zimmermann, A., Wolf, D.G., Saleh, N., Biton, M., Horwitz, E., Prokocimer, Z., Prichard, M., Hahn, G., et al. (2007). Host immune system gene targeting by a viral miRNA. Science *317*, 376–381.

Stern-Ginossar, N., Gur, C., Biton, M., Horwitz, E., Elboim, M., Stanietsky, N., Mandelboim, M., and Mandelboim, O. (2008). Human microRNAs regulate stress-induced immune responses mediated by the receptor NKG2D. Nat. Immunol. *9*, 1065–1073.

Tang, Y., Luo, X., Cui, H., Ni, X., Yuan, M., Guo, Y., Huang, X., Zhou, H., de Vries, N., Tak, P.P., Chen, S., and Shen, N. (2009). MicroRNA-146A contributes to abnormal activation of the type I interferon pathway in human lupus by targeting the key signaling proteins. Arthritis Rheum. *60*, 1065–1075.

Vigorito, E., Perks, K.L., Abreu-Goodger, C., Bunting, S., Xiang, Z., Kohlhaas, S., Das, P.P., Miska, E.A., Rodriguez, A., Bradley, A., et al. (2007). microRNA-155 regulates the generation of immunoglobulin class-switched plasma cells. Immunity *27*, 847–859.

Wang, S.E., Wu, F.Y., Chen, H., Shamay, M., Zheng, Q., and Hayward, G.S. (2004). Early activation of the Kaposi's sarcoma-associated herpesvirus RTA, RAP, and MTA promoters by the tetradecanoyl phorbol acetate-induced AP1 pathway. J. Virol. *78*, 4248–4267.

Weinmann, L., Hock, J., Ivacevic, T., Ohrt, T., Mutze, J., Schwille, P., Kremmer, E., Benes, V., Urlaub, H., and Meister, G. (2009). Importin 8 is a gene silencing factor that targets argonaute proteins to distinct mRNAs. Cell *136*, 496–507.

Xia, T., O'Hara, A., Araujo, I., Barreto, J., Carvalho, E., Sapucaia, J.B., Ramos, J.C., Luz, E., Pedroso, C., Manrique, M., et al. (2008). EBV microRNAs in primary lymphomas and targeting of CXCL-11 by ebv-mir-BHRF1-3. Cancer Res. *68*, 1436–1442.

Yang, I.V., Wade, C.M., Kang, H.M., Alper, S., Rutledge, H., Lackford, B., Eskin, E., Daly, M.J., and Schwartz, D.A. (2009a). Identification of novel genes that mediate innate immunity using inbred mice. Genetics *183*, 1535–1544.

Yang, Y., Chaerkady, R., Beer, M.A., Mendell, J.T., and Pandey, A. (2009b). Identification of miR-21 targets in breast cancer cells using a quantitative proteomic approach. Proteomics *9*, 1374–1384.

Yano, M., Hoogenraad, N., Terada, K., and Mori, M. (2000). Identification and functional analysis of human Tom22 for protein import into mitochondria. Mol. Cell. Biol. *20*, 7205–7213.

Ye, F.C., Zhou, F.C., Xie, J.P., Kang, T., Greene, W., Kuhne, K., Lei, X.F., Li, Q.H., and Gao, S.J. (2008). Kaposi's sarcoma-associated herpesvirus latent gene vFLIP inhibits viral lytic replication through NF-kappaB-mediated suppression of the AP-1 pathway: a novel mechanism of virus control of latency. J. Virol. *82*, 4235–4249.

Zhu, J.Y., Pfuhl, T., Motsch, N., Barth, S., Nicholls, J., Grasser, F., and Meister, G. (2009). Identification of novel Epstein-Barr virus microRNA genes from nasopharyngeal carcinomas. J. Virol. *83*, 3333–3341.

Ziegelbauer, J.M., Sullivan, C.S., and Ganem, D. (2009). Tandem array-based expression screens identify host mRNA targets of virus-encoded microRNAs. Nat. Genet. *41*, 130–134.